

Analysis and Design Trade-Offs for Power Network Inter-Area Oscillations

Xiaofan Wu, Florian Dörfler, and Mihailo R. Jovanović

Abstract—Conventional analysis and control approaches to inter-area oscillations in bulk power systems are based on a modal perspective. Typically, inter-area oscillations are identified from spatial profiles of poorly damped modes, and they are damped using carefully tuned decentralized controllers. To improve upon the limitations of conventional decentralized strategies, recent efforts aim at distributed wide-area control which involves the communication of remote signals. Here, we introduce a novel approach to the analysis and control of inter-area oscillations. Our framework is based on a stochastically driven system with performance outputs chosen such that the \mathcal{H}_2 norm is associated with incoherent inter-area oscillations. We show that an analysis of the output covariance matrix offers new insights relative to modal approaches. Next, we leverage the recently proposed sparsity-promoting optimal control approach to design controllers that use relative angle measurements and simultaneously optimize the closed-loop performance and the control architecture. For the IEEE 39 New England model, we investigate performance trade-offs of different control architectures and show that optimal retuning of decentralized control strategies can effectively guard against inter-areas oscillations.

I. INTRODUCTION

Inter-area oscillations in bulk power systems are associated with the dynamics of power transfers and involve groups of synchronous machines oscillating relative to each other. These system-wide oscillations arise from modular network topologies (with tightly clustered groups of machines and sparse interconnections among these clusters), heterogeneous machine dynamics (resulting in slow and fast responses), and large inter-area power transfers. As the system loading increases and renewables are deployed in remote areas, long-distance power transfers will outpace the addition of new transmission facilities. As a result, inter-area oscillations become ever more weakly damped, induce severe stress and performance limitations on the transmission network, and may even become unstable and cause outages [1]; see the 1996 Western U.S. blackout [2].

Traditional analysis and control approaches to inter-area oscillations are based on modal approaches [3], [4]. Typically, inter-area oscillations are identified from the spatial profiles of eigenvectors and participation factors of poorly damped modes [5], [6]. Such oscillations are conventionally

damped via decentralized controllers, whose gains are carefully tuned according to root locus criteria [7]–[9].

To improve upon the limitations of decentralized controllers, recent research efforts aim at distributed wide-area control strategies that involve the communication of remote signals, see the surveys [10], [11] and the excellent articles in [12]. The wide-area control signals are typically chosen to maximize modal observability metrics [13], [14], and the control design methods range from root locus criteria to robust and optimal control approaches [15]–[17].

Here, we investigate a novel approach to the analysis and control of inter-area oscillations. Our unifying analysis and control framework is based on a stochastically driven power system model with performance outputs inspired by slow coherency theory [18], [19]. We analyze inter-area oscillations by means of the \mathcal{H}_2 norm of this system, as in recent related approaches for interconnected oscillator networks and multi-machine power systems [20]–[22]. We show that an analysis of power spectral density and variance amplification offers new insights that complement conventional modal approaches.

To identify sparse wide-area control architecture and design optimal controllers, we appeal to the recently proposed paradigm of sparsity-promoting optimal control [23]–[26]. Sparsity-promoting control approaches have been successfully employed for wide-area control in power systems [27]–[29]. Here, we follow the sparsity-promoting optimal control framework developed in [30] and find a linear static state feedback that simultaneously optimizes a standard quadratic \mathcal{H}_2 optimal control criterion (associated with incoherent and poorly damped inter-area oscillations) and induces a sparse control architecture. Reference [30] augments the approach developed in [25] by imposing one additional structural constraint on the distributed controller. This structural constraint requires relative angle exchange between different generators, thereby preserving rotational symmetry of the original power system.

We investigate different performance indices resulting in controllers that strike a balance between low communication complexity and closed-loop performance. We are able to identify fully decentralized controllers that achieve comparable performance relative to the optimal centralized controllers. Thus, our results also provide a constructive answer to the much-debated question whether locally observable oscillations in a power network are also locally controllable; see [31]. This leads to a potential optimal feedback control design algorithm for retuning of the decentralized PSS gains to achieve better wide-area performance. We illustrate the

Financial support from the University of Minnesota Initiative for Renewable Energy and the Environment under Early Career Award RC-0014-11 and from University of California, Los Angeles Electrical Engineering Department start-up funds is gratefully acknowledged.

Xiaofan Wu and Mihailo R. Jovanović are with the Department of Electrical and Computer Engineering, University of Minnesota, Minneapolis, MN 55455. Emails: [wuxxx836, mihailo]@umn.edu. F. Dörfler is with the Automatic Control Laboratory at ETH Zürich, Switzerland. Email: dorfler@control.ee.ethz.ch.

utility of our approach with the IEEE 39 New England power grid model, whose data can be found in [32].

The remainder of this paper is organized as follows. In Section II-A, we briefly summarize the model and highlight causes for inter-area oscillations in power networks. In Section II-B, we utilize power spectral density and variance amplification analyses to provide new insights into inter-area oscillations. In Section II-C, we formulate the sparsity-promoting optimal control problem subject to structural constraints on relative angle information exchange. In Section III, we present our control design and examine performance of open- and closed-loop systems for the IEEE 39 New England power grid. Finally, in Section IV, we conclude the paper.

II. PROBLEM FORMULATION

A. Modeling and background on inter-area oscillations

A power network is described by the nonlinear system of differential-algebraic equations. Differential equations govern the dynamics of generators and their control equipments, and the algebraic equations describe load flow, generator stator, and power electronic components [33]. After linearization around a stationary operating point and elimination of the algebraic equations, we obtain a linear state-space model

$$\dot{x} = Ax + B_1 d + B_2 u. \quad (1)$$

Here, x is the state, u is the control input provided by generator excitation/governor control or power electronics devices, and d is the white-noise disturbance which may arise from fluctuations in renewable generation and uncertain load demand [33], [34].

The dominant dynamical behavior of a multi-machine power system typically arises from the electro-mechanical interactions among the generators and it is captured by the *swing equation* [33],

$$M\ddot{\theta} + D\dot{\theta} + L\theta = 0. \quad (2)$$

This equation does not account for control and disturbance inputs and it is obtained by neglecting the fast electrical dynamics. Here, θ and $\dot{\theta}$ are the generator rotor angles and frequencies, M and D are the diagonal matrices of generator inertia and damping coefficients, and L is a Laplacian matrix that describes the interactions between generators [28]. The swing dynamics (2) feature an inherent *rotational symmetry* and are invariant under a rigid rotation of all angles θ .

The swing equations (2) describe a system of heterogenous oscillators which are harmonically coupled through a spring-type network with Laplacian matrix L . Inter-area oscillations arise when densely connected groups of generators (so-called areas) are sparsely connected with each other. These areas can be aggregated into coherent groups of machines which swing relative to each other using the slow coherency analysis [18], [19].

In this paper, we design wide-area controllers to suppress such inter-area oscillations. With a linear static state-

feedback, $u = -Gx$, the closed-loop system takes the form

$$\begin{aligned} \dot{x} &= (A - B_2 G)x + B_1 d \\ z &= \begin{bmatrix} z_1 \\ z_2 \end{bmatrix} = \begin{bmatrix} Q^{1/2} \\ -R^{1/2} G \end{bmatrix} x \end{aligned} \quad (3)$$

where z is a performance output with state and control weights Q and R . The preceding discussion on inter-area oscillations suggests that homogeneous networks (with identical all-to-all coupling among generators) feature no inter-area oscillations. This suggests a state objective of the form

$$x^T Q x = \frac{1}{2} \theta^T L_{\text{unif}} \theta + \frac{1}{2} \dot{\theta}^T M \dot{\theta}$$

where L_{unif} is the uniform Laplacian (or projector) matrix

$$L_{\text{unif}} = I - (1/N) \mathbb{1} \mathbb{1}^T \quad (4)$$

and $\mathbb{1}$ is the vectors of all ones. The objective function $x^T Q x$ quantifies the kinetic and potential energy of the swing dynamics in a homogeneous network, and it preserves rotational symmetry. The term $u^T R u$ quantifies the control effort; for simplicity, we choose the control weight R to be the identity matrix.

B. Power spectral density and variance amplification

The conventional analysis of inter-area oscillations in power systems is based on spatial profiles of eigenvectors and participation factors of poorly damped modes. Similarly, the traditional control design is based on a modal perspective [5], [6]. In this paper, we quantify performance of both open- and closed-loop systems using power spectral density and variance amplification analyses. This approach offers additional and complementary insights to a modal analysis. More specifically, an eigenvalue decomposition of the output covariance matrix reveals the sources of variance amplification, and a power spectral density analysis reveals the dominant frequencies corresponding to the inter-area modes.

We briefly review the power spectral density and variance amplification analysis of a linear state space system of the form (3). The \mathcal{H}_2 norm from the white noise input d to the performance output z is defined as [35]

$$\begin{aligned} \|H(j\omega)\|_2^2 &= \frac{1}{2\pi} \int_{-\infty}^{\infty} \|H(j\omega)\|_{HS}^2 d\omega \\ &= \text{trace}(X(Q + G^T R G)) \end{aligned} \quad (5)$$

where $H(j\omega)$ is the frequency response from d to z , and the controllability Gramian X is the solution to the Lyapunov equation [35]

$$(A - B_2 G)X + X(A - B_2 G)^T = -B_1 B_1^T. \quad (6)$$

The Hilbert-Schmidt norm quantifies the power spectral density of the stochastically forced system (3),

$$\begin{aligned} \|H(j\omega)\|_{HS}^2 &= \text{trace}(H(j\omega)H^*(j\omega)) \\ &= \sum_i \sigma_i^2(H(j\omega)) \end{aligned} \quad (7)$$

where the σ_i 's are the singular values of $H(j\omega)$.

The controllability Gramian X in (6) is also the steady-state covariance matrix of the state x , and

$$Y = Q^{1/2} X Q^{1/2}$$

is the steady-state covariance matrix of the output z_1 . The eigenvalue decomposition of the matrix Y ,

$$Y = \sum_i \lambda_i v_i v_i^T \quad (8)$$

provides insight about relative roles of different modes in the variance amplification. Since the total variance amplification from d to z_1 is determined by the sum of the eigenvalues λ_i of Y , each mode v_i contributes λ_i to the total variance amplification. Thus, the spatial structure of the mode that contributes most to the variance amplification is determined by the principal eigenvector of the matrix Y , v_1 .

C. Sparsity-promoting linear quadratic control with structural constraints

The sparsity-promoting optimal control framework developed in [23], [25] aims at finding a static state feedback G that simultaneously optimizes the \mathcal{H}_2 norm of system (3) and induces a sparse control architecture. Compared to conventional optimal control and stabilization problems, as a result of the rotational symmetry, both the open-loop matrix A and the state performance weight Q feature a common zero eigenvalue with identical eigenvector associated with the average of all rotor angles. In earlier work [27], [28], to arrive at a stabilizing and numerically feasible solution, we have removed the natural rotational symmetry by adding a small *regularization* term to the diagonal elements of the performance matrix Q . The resulting controllers require the use of absolute angle measurements (with respect to a common reference) to stabilize the average rotor angle. Furthermore, such a regularization induces a slack bus (a reference generator with fixed angle) and thereby changes structure of the original network.

In this article, we restrict our attention to only relative rotor angle measurements which preserve the natural network symmetries. Note that this requirement imposes additional structural constraints on the feedback gain G : the average rotor angle has to remain invariant under the state feedback $u = -Gx$. To cope with these structural constraints, the approach of [25] has been recently augmented in [30].

Following [30], we introduce the orthonormal coordinate transformation

$$T = \begin{bmatrix} U & 0 \\ 0 & I \end{bmatrix}$$

where the columns of the matrix $U \in \mathbb{R}^{N \times (N-1)}$ form an orthonormal basis for the subspace $\mathbb{1}^\perp$, and N denotes the number of generators. For example, the columns of U can be obtained from the $(N-1)$ eigenvectors of the matrix L_{unif} in (4) corresponding to the non-zero eigenvalues. In the new set of coordinates, the matrices of the closed-loop system (3)

change to

$$\bar{A} := T^T A T, \quad \bar{B}_i := T^T B_i, \quad \bar{Q}^{1/2} := Q^{1/2} T.$$

The feedback matrices G (in the original set of coordinates) and F (in the new set of coordinates) are related by

$$F = G T \Leftrightarrow G = F T^T.$$

The \mathcal{H}_2 norm from d to z is then obtained as

$$J(F) := \begin{cases} \text{trace}(\bar{B}_1^T P(F) \bar{B}_1) & \text{for } F \text{ stabilizing} \\ \infty & \text{otherwise} \end{cases}$$

where $P(F)$ is the closed-loop observability Gramian that satisfies the Lyapunov equation

$$(\bar{A} - \bar{B}_2 F)^T P + P(\bar{A} - \bar{B}_2 F) = -(\bar{Q} + F^T \bar{R} F).$$

The objective is to achieve a desirable tradeoff between the \mathcal{H}_2 performance of the closed-loop system and the sparsity of the feedback gain. While the \mathcal{H}_2 performance is expressed in terms of the matrix F in the new set of coordinates, it is desired to enhance sparsity of the matrix G in the original set of coordinates. In order to achieve this task, the following sparsity-promoting optimal control problem has been formulated in [30],

$$\begin{aligned} & \text{minimize} && J(F) + \gamma g(G) \\ & \text{subject to} && F T^T - G = 0. \end{aligned} \quad (9)$$

The non-negative parameter γ determines the emphasis on sparsity, and the regularization term is given by the weighted ℓ_1 -norm of G ,

$$g(G) := \sum_{i,j} W_{ij} |G_{ij}|.$$

In [30], the alternating direction method of multipliers (ADMM) algorithm [36] was used to efficiently solve the optimization problem (9). We refer the reader to [25], [30] for algorithmic details.

III. CASE STUDY: IEEE 39 NEW ENGLAND EXAMPLE

We consider the IEEE 39 New England Power Grid Model. This system is illustrated in Fig. 1 and it consists of 39 buses and 10 detailed two-axis generator models. Generators 1 to 9 are equipped with excitation control systems, and generator 10 is an equivalent aggregated model representing a neighboring transmission network area. In this example, all loads are modeled as constant power loads.

We follow a two-level control strategy that combines local and wide-area control. The local control inputs are used to suppress local oscillations and they are based on a conventional power system stabilizer (PSS) design; the wide-area controller is designed to damp inter-area oscillations. For the local control, we use a standard PSS controller with lead/lag elements and carefully tuned coefficients taken from [9]; see [28] for further details. For the subsequent analysis and the wide-area control design, we assume that the local PSS controllers are embedded in the open-loop system matrix A .

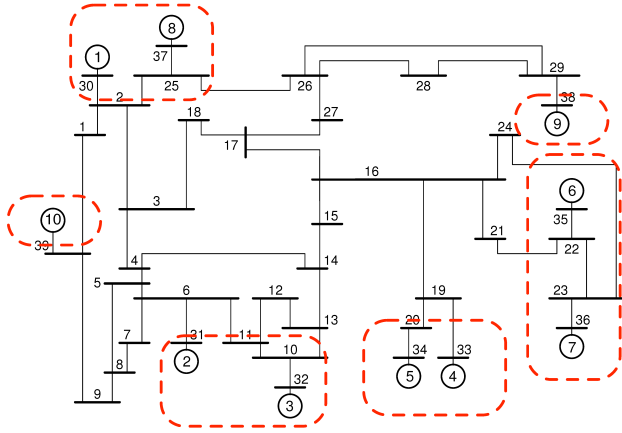


Fig. 1: IEEE 39 New England Power Grid and its groups of coherent machines

A. Analysis of the open-loop system

Despite the action of the local PSS controllers, modal and participation factor analyses reveal the presence of five dominant inter-area modes in the open-loop New England power grid model [28]. These modes are reported in Table I, and the groups of coherent machines (identified from the spatial profiles of eigenvectors) are illustrated in Fig. 1. This spatial profile together with modal controllability and observability metrics was previously used to indicate which wide-area controller links need to be added to dampen or distort the inter-area modes [13], [14].

Here, we depart from this modal perspective and follow a different path. We first examine the power spectral density and variance amplification of the open-loop system. This type of analysis allows us to identify the temporal frequencies for which large amplification occurs and spatial structure of strongly amplified responses. We note that in general these do not correspond to the spatial profiles of the weakly-damped system modes.

TABLE I: Inter-area modes of the New England power grid

mode no.	eigenvalue pair	damping ratio	frequency [Hz]	coherent groups
1	$-0.6347 \pm i 3.7672$	0.16614	0.59956	10 vs. all others
2	$-0.7738 \pm i 6.7684$	0.11358	1.0772	1,8 vs. 2-7,9,10
3	$-1.1310 \pm i 5.7304$	0.19364	0.91202	1,2,3,8,9 vs. 4-7
4	$-1.1467 \pm i 5.9095$	0.19049	0.94052	4,5,6,7,9 vs. 2,3
5	$-1.5219 \pm i 5.8923$	0.25009	0.93778	4,5 vs. 6,7

Figure 2 illustrates the power spectral density of the open-loop system. While the largest amplification occurs for small temporal frequencies, we observe two resonant peaks. The first peak at $\omega_1 = 5.7882$ rad/s ($f_1 = \omega_1/2\pi = 0.9212$ Hz) corresponds to the inter-area modes 2, 3, 4, 5 in Table I. The second peak at $\omega_2 = 3.7896$ rad/s ($f_2 = \omega_2/2\pi = 0.5996$ Hz) corresponds to inter-area mode 1 in Table I.

Next, we study the contribution of each generator to the variance amplification and examine the spatial structure of

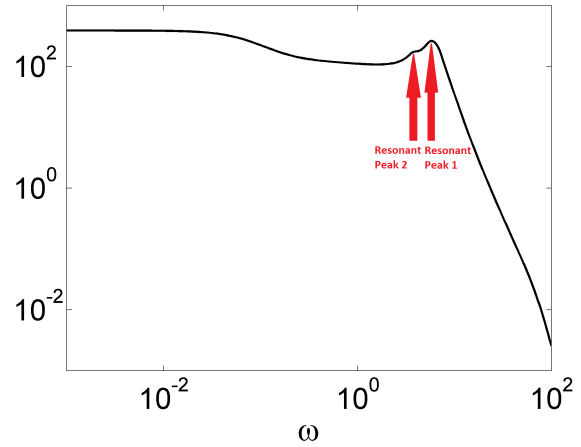


Fig. 2: Power spectral density of the open-loop system.

the modes of the output covariance matrix Y for the open-loop system. In Fig. 3, the diagonal elements of the output covariance matrix show variances of angles and frequencies of the individual generators. We see that frequencies are better aligned than angles and conclude that the bulk of the variance amplification arises from the misalignment of angles of generators 4, 5, 8 and 9. A similar observation can be made from Fig. 4 which displays the eigenvectors corresponding to the four largest eigenvalues of the open-loop output covariance matrix Y . We note that in Figs. 3 and 4, the first 10 indices correspond to angles and the remaining ones correspond to frequencies.

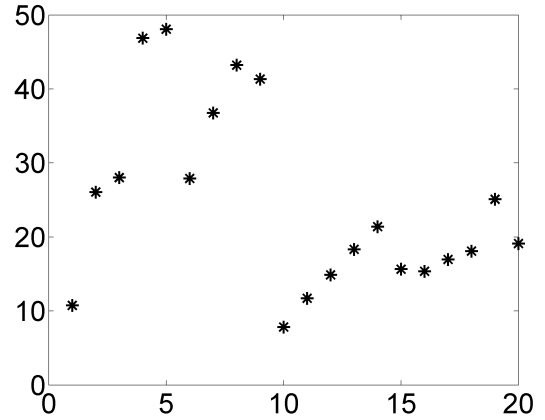


Fig. 3: Diagonal elements of open-loop covariance matrix Y .

In summary, the eigenvalue analysis of the output covariance matrix provides important insights into the sources of variance amplification. Since sparsity-promoting \mathcal{H}_2 optimal control design is based on minimizing the variance amplification, our framework can also be used to explain the sparsity pattern of the resulting controllers. In what follows, we illustrate why the addition of certain long-range communication links can improve the closed-loop performance.

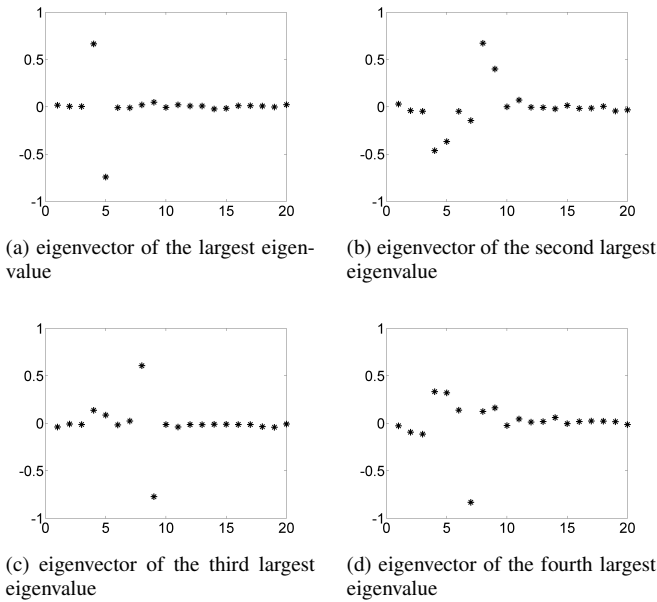


Fig. 4: Eigenvectors corresponding to the four largest eigenvalues of the covariance matrix Y of the open-loop system.

B. Sparsity-promoting optimal control

We use sparsity-promoting optimal control formulation (9) with 100 logarithmically-spaced points for $\gamma = [10^{-4}, 2]$. In Fig. 5, sparsity patterns of the feedback matrix G for different values of γ are illustrated. When $\gamma = 0.1099$, controller on generator 9 needs to have access to the rotor angles of generator 5 and the aggregated model 10. This wide-area control architecture is not surprising since generator 9 is the least connected generator (in terms of the effective resistance metric, see [37]), the aggregated model 10 dominates¹ the power system’s kinetic energy $1/2 \dot{\theta}^T M \dot{\theta}$, and generator 5 dominates the most energetic coherent group consisting of generators 4 and 5 (see the spatial distribution in Figs. 3 and 4) in terms of angle misalignment. For $\gamma = 0.4460$, we obtain a fully-decentralized controller, and performance is compromised by about 7.5% relative to the optimal centralized controller; see Fig. 6. By increasing γ to 2, the performance is compromised by about 10.5%.

We emphasize that we can embed our fully decentralized controller into the local generator excitation control systems. For example, this can be done by directly feeding the decentralized and local state-feedback to the automatic voltage regulator or by retuning the gains of the existing local PSS controllers. In other words, inter-area oscillations can be suppressed by purely local control strategies while achieving nearly the same performance of the optimal centralized controller.

¹The inertia of the aggregated equivalent model 10 is an order of magnitude larger than those of the physical generators 1, . . . , 9.

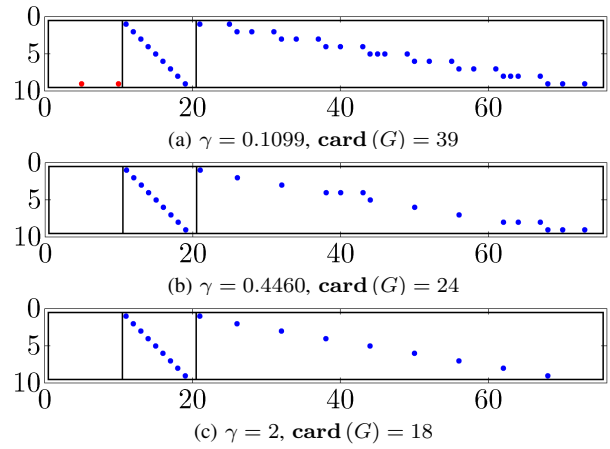


Fig. 5: Sparsity pattern of G .

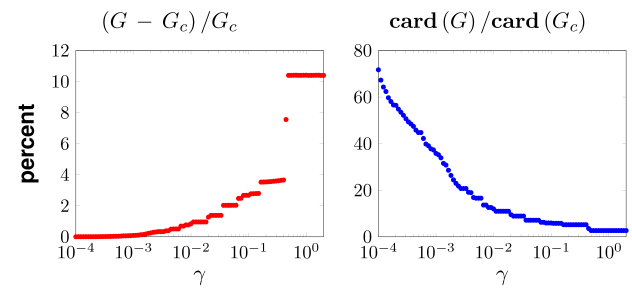


Fig. 6: Performance vs sparsity comparison relative to the optimal centralized controller G_c .

C. Comparison of open-loop and closed-loop systems

The structure of the sparsity-promoting controller with $\gamma = 2$ is shown in Fig. 5c. This controller is fully decentralized with only 18 nonzero elements. In this section, we compare the power spectral density and variance amplification of the following three systems: the open-loop system, the closed-loop system with optimal centralized controller, and the closed-loop system with the sparse decentralized controller depicted in Fig. 5c.

Figure 7 provides a comparison between the power spectral densities of three cases. The fully decentralized sparse controller performs almost as well as the optimal centralized controller for high frequencies; for low frequencies, we observe some discrepancy that accounts for about 10% of performance degradation in the variance amplification.

In Fig. 8, we plot the eigenvalues of the output covariance matrix Y for the three cases mentioned above. Relative to the open-loop system, both the optimal centralized and the decentralized feedback gains significantly reduce the variance amplification. The diagonal elements of the output covariance matrix for all three cases are shown in Fig. 9. We observe that our control strategy is capable of diminishing the variance of both angles and frequencies. Additionally, the diagonal elements of the output covariance matrix are equalized and balanced by both the optimal centralized and

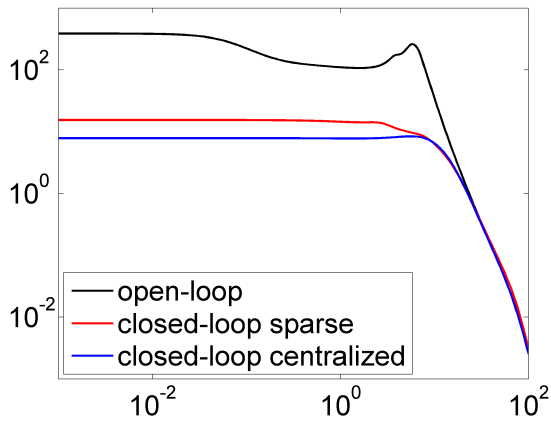


Fig. 7: Power spectral density comparison.

the decentralized controller. We conclude that, similar to the modal observations discussed in [28], the optimal feedback gain not only increases the damping of the eigenvalues associated with the inter-area modes, but it structurally distorts these modes by rotating the corresponding eigenvectors.

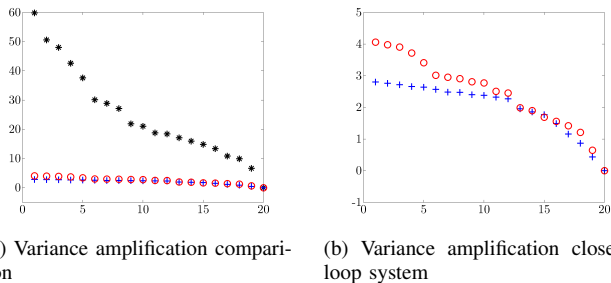


Fig. 8: Variance amplification comparison. *’s represent open-loop system, \circ ’s represent closed-loop system with sparse decentralized controller, and +’s represent closed-loop system with optimal centralized controller.

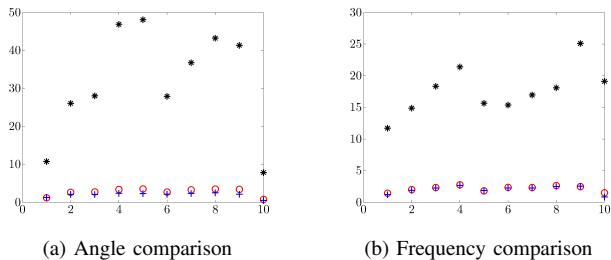


Fig. 9: Variances of angles and frequencies of different generators.

IV. CONCLUDING REMARKS

In this paper, we have analyzed inter-area oscillations of power systems by studying their power spectral density

functions and output covariance matrices. Our analysis of the open-loop system identifies the root cause for inter-area oscillations. By comparing performance of open- and closed-loop systems, we have been able to understand the effect of the sparsity-promoting control both in terms of performance and with regards to the resulting closed-loop communication pattern. For the IEEE 39 New England model, we have provided a systematic method for optimal retuning of the decentralized PSS gains that leads to nearly the same performance levels as the optimal centralized controller.

REFERENCES

- [1] F. Alvarado, C. DeMarco, I. Dobson, P. Sauer, S. Greene, H. Engdahl, and J. Zhang, "Avoiding and suppressing oscillations," *PSERC Project Final Report*, 1999.
- [2] V. Venkatasubramanian and Y. Li, "Analysis of 1996 Western American electric blackouts," in *Bulk Power System Dynamics and Control-VI*, Cortina d'Ampezzo, Italy, 2004.
- [3] K. Prasertwong, N. Mithulananthan, and D. Thakur, "Understanding low-frequency oscillation in power systems," *International Journal of Electrical Engineering Education*, vol. 47, no. 3, pp. 248–262, 2010.
- [4] L. Rouco, "Eigenvalue-based methods for analysis and control of power system oscillations," in *Power System Dynamics Stabilisation, IEE Colloquium on*. IET, 1998.
- [5] G. Rogers, "Demystifying power system oscillations," *Computer Applications in Power, IEEE*, vol. 9, no. 3, pp. 30–35, 1996.
- [6] M. Klein, G. Rogers, and P. Kundur, "A fundamental study of inter-area oscillations in power systems," *Power Systems, IEEE Transactions on*, vol. 6, no. 3, pp. 914–921, 1991.
- [7] M. Klein, G. Rogers, S. Moorthy, and P. Kundur, "Analytical investigation of factors influencing power system stabilizers performance," *Energy Conversion, IEEE Transactions on*, vol. 7, no. 3, pp. 382–390, 1992.
- [8] N. Martins and L. T. G. Lima, "Eigenvalue and frequency domain analysis of small-signal electromechanical stability problems," in *IEEE/PES Symposium on Applications of Eigenanalysis and Frequency Domain Methods*, 1989, pp. 17–33.
- [9] R. A. Jabr, B. C. Pal, N. Martins, and J. C. R. Ferraz, "Robust and coordinated tuning of power system stabiliser gains using sequential linear programming," *IET Generation, Transmission & Distribution*, vol. 4, no. 8, pp. 893–904, 2010.
- [10] J. Xiao, F. Wen, C. Y. Chung, and K. P. Wong, "Wide-area protection and its applications—a bibliographical survey," in *IEEE PES Power Systems Conference and Exposition*, Atlanta, GA, USA, Oct. 2006, pp. 1388–1397.
- [11] K. Seethalekshmi, S. N. Singh, and S. C. Srivastava, "Wide-area protection and control: Present status and key challenges," in *Fifteenth National Power Systems Conference*, Bombay, India, Dec. 2008, pp. 169–175.
- [12] M. Amin, "Special issue on energy infrastructure defense systems," *Proceedings of the IEEE*, vol. 93, no. 5, pp. 855–860, 2005.
- [13] A. Heniche and I. Karnwa, "Control loops selection to damp inter-area oscillations of electrical networks," *IEEE Transactions on Power Systems*, vol. 17, no. 2, pp. 378–384, 2002.
- [14] L. P. Kunjumammed, R. Singh, and B. C. Pal, "Robust signal selection for damping of inter-area oscillations," *IET Generation, Transmission & Distribution*, vol. 6, no. 5, pp. 404–416, 2012.
- [15] G. E. Boukarim, S. Wang, J. H. Chow, G. N. Taranto, and N. Martins, "A comparison of classical, robust, and decentralized control designs for multiple power system stabilizers," *IEEE Transactions on Power Systems*, vol. 15, no. 4, pp. 1287–1292, 2000.
- [16] Y. Zhang and A. Bose, "Design of wide-area damping controllers for interarea oscillations," *IEEE Transactions on Power Systems*, vol. 23, no. 3, pp. 1136–1143, 2008.
- [17] M. Zima, M. Larsson, P. Korba, C. Rehtanz, and G. Andersson, "Design aspects for wide-area monitoring and control systems," *Proceedings of the IEEE*, vol. 93, no. 5, pp. 980–996, 2005.
- [18] J. H. Chow and P. Kokotović, "Time scale modeling of sparse dynamic networks," *IEEE Transactions on Automatic Control*, vol. 30, no. 8, pp. 714–722, 1985.

- [19] D. Romeres, F. Dörfler, and F. Bullo, "Novel results on slow coherency in consensus and power networks," in *European Control Conference*, Zürich, Switzerland, July 2013, to appear.
- [20] B. Bamieh, M. R. Jovanović, P. Mitra, and S. Patterson, "Coherence in large-scale networks: dimension dependent limitations of local feedback," *IEEE Trans. Automat. Control*, vol. 57, no. 9, pp. 2235–2249, September 2012.
- [21] B. Bamieh and D. F. Gayme, "The price of synchrony: Resistive losses due to phase synchronization in power networks," 2012, arXiv:1209.6579.
- [22] M. Fardad, F. Lin, and M. R. Jovanović, "Design of optimal sparse interconnection graphs for synchronization of oscillator networks," *IEEE Trans. Automat. Control*, 2014, doi:10.1109/TAC.2014.2301577.
- [23] M. Fardad, F. Lin, and M. R. Jovanović, "Sparsity-promoting optimal control for a class of distributed systems," in *Proceedings of the 2011 American Control Conference*, San Francisco, CA, 2011, pp. 2050–2055.
- [24] F. Lin, M. Fardad, and M. R. Jovanović, "Sparse feedback synthesis via the alternating direction method of multipliers," in *Proceedings of the 2012 American Control Conference*, Montréal, Canada, 2012, pp. 4765–4770.
- [25] F. Lin, M. Fardad, and M. R. Jovanović, "Design of optimal sparse feedback gains via the alternating direction method of multipliers," *IEEE Trans. Automat. Control*, vol. 58, no. 9, pp. 2426–2431, 2013.
- [26] S. Schuler, U. Münz, and F. Allgöwer, "Decentralized state feedback control for interconnected process systems," in *IFAC Symposium on Advanced Control of Chemical Processes*, Furama Riverfront, Singapore, July 2012, pp. 1–10.
- [27] F. Dörfler, M. R. Jovanović, M. Chertkov, and F. Bullo, "Sparse and optimal wide-area damping control in power networks," in *American Control Conference*, Washington, DC, USA, June 2013, pp. 4295–4300.
- [28] F. Dörfler, M. R. Jovanović, M. Chertkov, and F. Bullo, "Sparsity-promoting optimal wide-area control of power networks," *IEEE Trans. Power Syst.*, 2014, doi:10.1109/TPWRS.2014.2304465.
- [29] S. Schuler, U. Münz, and F. Allgöwer, "Decentralized state feedback control for interconnected systems with application to power systems," *Journal of Process Control*, vol. 24, no. 2, pp. 379–388, 2014.
- [30] X. Wu and M. R. Jovanović, "Sparsity-promoting optimal control of consensus and synchronization networks," in *Proceedings of the 2014 American Control Conference*, Portland, OR, 2014, to appear.
- [31] B. E. Eliasson and D. J. Hill, "Damping structure and sensitivity in the NORDEL power system," *IEEE Transactions on Power Systems*, vol. 7, no. 1, pp. 97–105, 1992.
- [32] J. H. Chow and K. W. Cheung, "A toolbox for power system dynamics and control engineering education and research," *IEEE Transactions on Power Systems*, vol. 7, no. 4, pp. 1559–1564, 1992.
- [33] P. Kundur, *Power system stability and control*. McGraw-Hill, 1994.
- [34] P. M. Anderson and A. A. Fouad, *Power system control and stability*. Wiley, 2008.
- [35] G. E. Dullerud and F. Paganini, *A course in robust control theory*. Springer, 2000.
- [36] S. Boyd, N. Parikh, E. Chu, B. Peleato, and J. Eckstein, "Distributed optimization and statistical learning via the alternating direction method of multipliers," *Foundations and Trends in Machine Learning*, vol. 3, no. 1, pp. 1–124, 2011.
- [37] F. Dörfler and F. Bullo, "Kron reduction of graphs with applications to electrical networks," *IEEE Transactions on Circuits and Systems I: Regular Papers*, vol. 60, no. 1, pp. 150–163, 2013.